The Potent Anti-HIV Protein Cyanovirin-N Contains Two Novel Carbohydrate Binding Sites That Selectively Bind to Man_8 D1D3 and Man_9 with Nanomolar Affinity: Implications for Binding to the HIV Envelope Protein gp120

Carole A. Bewley* and Sarah Otero-Quintero

Contribution from the Laboratory of Bioorganic Chemistry, National Institute of Diabetes and Digestive and Kidney Diseases, National Institutes of Health, Bethesda, Maryland 20892-0820

Received November 21, 2000. Revised Manuscript Received February 20, 2001

Abstract: Cyanovirin-N (CVN) is a monomeric 11 kDa cyanobacterial protein that potently inactivates diverse strains of human immunodeficiency virus (HIV) at the level of cell fusion by virtue of high affinity interactions with the surface envelope glycoprotein gp120. Several lines of evidence have suggested that CVN−gp120 interactions are in part mediated by N-linked complex carbohydrates present on gp120, but experimental evidence has been lacking. To this end we screened a comprehensive panel of carbohydrates which represent structurally the N-linked carbohydrates found on gp120 for their ability to inhibit the fusion-blocking activity of CVN in a quantitative HIV-1 envelope-mediated cell fusion assay. Our results show that CVN specifically recognizes with nanomolar affinity $Man_9GlcNAc_2$ and the D1D3 isomer of $Man_8GlcNAc_2$. Nonlinear least squares best fitting of titration data generated using the cell fusion assay show that CVN binds to gp120 with an equilibrium association constant (K_a) of 2.4 (± 0.1) × 10^7 M^{-1} and an apparent stoichiometry of 2 equiv of CVN per gp120, $Man_8GlcNAc_2$ D1D3 acts as a divalent ligand (2 CVN:1 Man_8) with a K_a of 5.4 (± 0.5) × 10^7 M^{-1}, and $Man_9GlcNAc_2$ functions as a trivalent ligand (3 CVN:1 Man_9) with a K_a of 1.3 (± 0.3) × 10^8 M^{-1}. Isothermal titration calorimetry experiments of CVN binding to $Man_9GlcNAc_2$ at micromolar concentrations confirmed the nanomolar affinity (K_a = 1.5 (± 0.9) × 10^8 M^{-1}), and the fitted data indicated a stoichiometry equal to approximately one (1 Man_9:1 CVN). The 1:1 stoichiometry at micromolar concentrations suggested that CVN has not only a high affinity binding site—relevant to the studies at nM concentrations—but a lower affinity site as well that facilitates cross-linking of CVN-oligomannose at micromolar concentrations or higher. The specificity of CVN for Man_8 D1D3 and Man_9 over the D1D2 isomer of Man_8 indicated that the minimum structure required for high affinity binding comprises Manα1 → 2Manα. By following the $^1H-^{15}N$ correlation spectrum of ^{15}N-labeled CVN upon titration with this disaccharide, we unambiguously demonstrate that CVN recognizes and binds to the disaccharide Manα1 → 2Manα via two distinct binding sites of differing affinities located on opposite ends of the protein. The high affinity site has a K_a of 7.2 (± 4) × 10^6 M^{-1} and the low affinity site a K_a of 6.8 (± 4) × 10^5 M^{-1} as determined by isothermal titration calorimetry. Mapped surfaces of the carbohydrate binding sites are presented, and implications for binding to gp120 are discussed.

Introduction

Protein−carbohydrate interactions play a central role in myriad cellular processes and recognition events including viral and microbial pathogenesis, inflammation, and fertilization. Deciphering the structural basis of such events is of significant importance, especially from the perspective of chemical intervention of deleterious processes governed by such interactions. One very relevant example is that of the human immunodeficiency virus (HIV),[1] an enveloped virus whose surface is largely covered by carbohydrates. The initial steps in HIV infection include binding of the HIV surface envelope glycoprotein gp120 to CD4, which triggers conformational changes in gp120 to allow for subsequent interactions with the chemokine receptors CXCR4 and CCR5. The assembly of this complex ultimately facilitates virus−cell or cell−cell fusion (reviewed in ref 2). Cyanovirin-N (CVN) is a cyanobacterial protein that potently inactivates all strains of HIV and simian immunodeficiency virus (SIV) at the level of envelope-mediated fusion by virtue of its strong interactions with the HIV surface envelope (Env) glycoprotein gp120[3] and is currently under preclinical investigation as a topical antiviral microbicide.[4,5] High resolution structures have been solved for the naturally occurring monomer by NMR[6] (Figure 1a) and for the domain-swapped dimer by

(1) The abbreviations used are as follows: HIV, SIV, and FIV are human, simian, and feline immunodeficiency viruses, respectively; Env, viral envelope glycoproteins; gp120, 120 kDa surface envelope glycoprotein of HIV; gp41, 41 kDa transmembrane subunit of HIV envelope; CVN, cyanovirin-N; NMR, nuclear magnetic resonance spectroscopy; Man_n, Man_n-$GlcNAc_2$, eqivalent to oligomannose-*n* and used interchangeably throughout text; ITC, isothermal titration calorimetry; Manα1, α-D-mannopyranose; β-Gal, β-galactosidase.

(2) Chan, D. S.; Kim, P. *Cell* **1998**, *93*, 681−684.

(3) Boyd, M. R.; Gustafson, K. R.; McMahon, J. B.; Shoemaker, R. H.; O'Keefe, B. R.; Mori, T.; Gulakowski, R. J.; Wu, L.; Rivera, M. I.; Laurencot, C. M.; Currens, M. J.; Cardellina, J. H.; Buckheit, R. W.; Nara, P. L.; Pannell, L. K.; Sowder, R. C.; Henderson, L. E. *Antimicrob. Agents Chemother.* **1997**, *41*, 1521−1530.

(4) Esser, M. T., Mori, T., Mondor, I., Sattentau, Q. J.; Dey, B.; Berger, E. A.; Boyd, M. R.; Lifson, J. D. *J. Virol.* **1999**, *73*, 4360−4371.

(5) Dey, B.; Lerner, D. L.; Lusso, P.; Boyd, M. R.; Elder, J. H.; Berger, E. A. *J. Virol.* **2000**, *74*, 4562−4569.

10.1021/ja004040e
Published on Web 04/04/2001

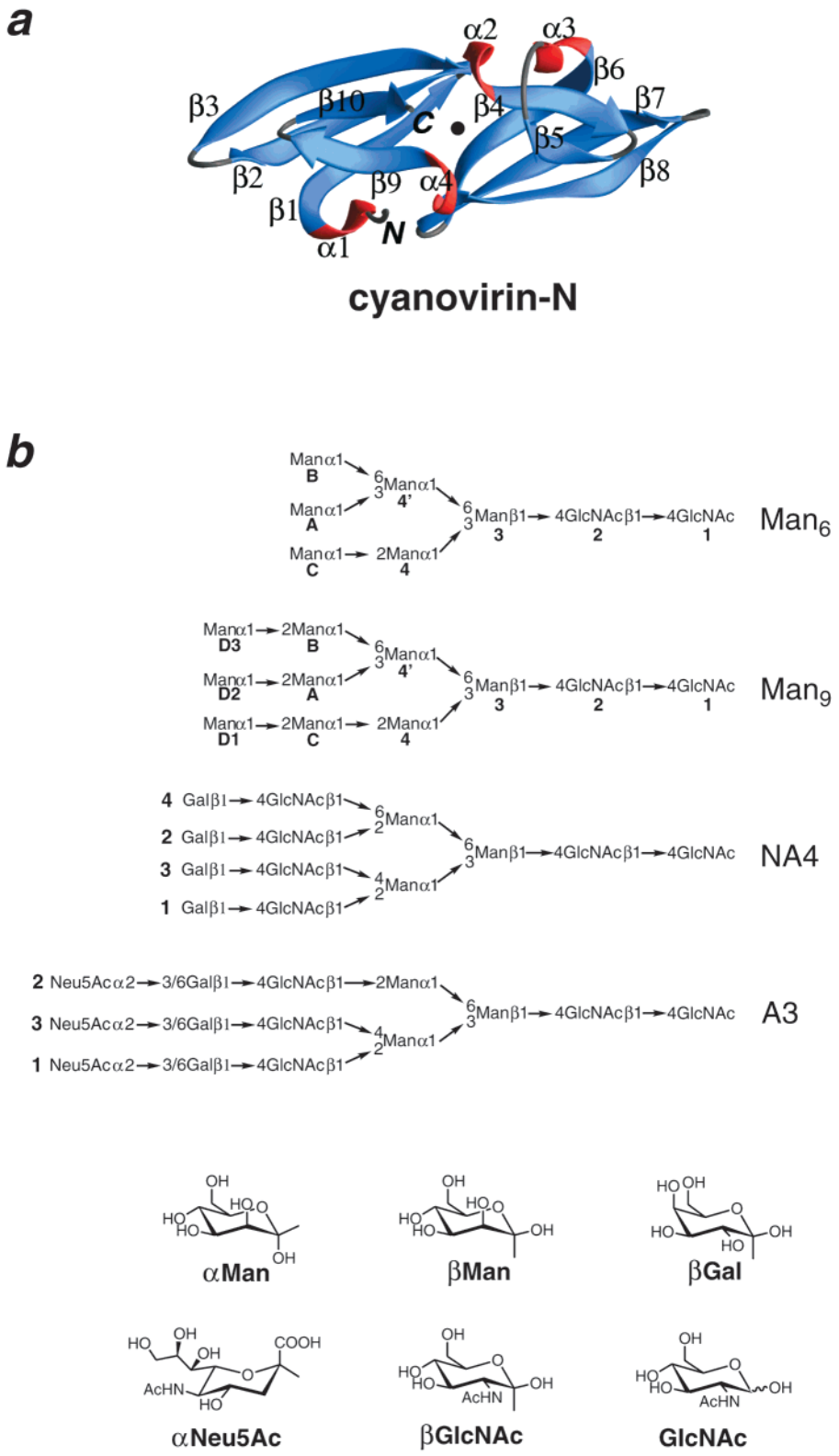

Figure 1. Structures of cyanovirin-N and oligosaccharides. (a) Ribbon diagram of cyanovirin-N where β-sheets are colored blue, 3_{10}-helices are red, and coils are gray, and the centered black circle indicates the C_2 axis of pseudo-symmetry (PDB accession number 2EZM);[6] figure generated with the program MOLMOL.[35] (b) Formulas of N-linked oligomannose-type (Man_n) and complex-type carbohydrates present on the HIV surface envelope glycoprotein gp120. The formulas for Man_6 and Man_9 are shown where labels indicate standard numbering of monosaccharides in Man_9, and the three arms are labeled with standard notation as D1, D2, and D3; isomers of Man_7 and Man_8 can be deduced by adding appropriate mannopyranose termini to the structure of Man_6. Similarly, NA4 illustrates asialo multiantennary complex-type oligosaccharides and A3 represents sialylated multiantennary complex-type oligosaccharides with branch numbering printed at left. Chemical structures of the individual monosaccharides comprising N-linked oligosaccharides are shown in the bottom panel for reference.

X-ray crystallography at low pH[7] and by NMR at neutral pH.[8] Biochemical studies addressing the mechanism behind the potent antiviral activity of CVN have included binding,[9,10] hybridization,[4] and mutagenesis[11] studies and most recently investigations

into the activity of CVN at discrete steps along the HIV-1 Env-mediated fusion pathway.[5] All of these studies confirmed the initial finding that CVN interacts with gp120 (and not with CD4 or chemokine coreceptors) with high affinity and that these interactions are responsible for its potent antiviral activity. In addition to HIV, SIV, and FIV (feline immunodeficiency virus), CVN has been shown to potently inhibit several other, but not all, diverse strains of enveloped viruses, including measles virus and human herpes virus 6.[5]

Several lines of evidence have suggested that complex carbohydrates present on gp120 may play a role in CVN−gp120 binding. CVN binds to wild-type gp120 and the transmembrane subunit of Env (gp41) with much greater affinity than the nonglycosylated recombinant forms of these HIV envelope proteins.[3,10] (Interestingly, gp41 contains sequence coding for N-linked glycosylation only.[12]) Moreover, hybridization experiments employing monoclonal antibodies (MAbs) to defined epitopes on gp120 showed that CVN binding occludes subsequent binding of only one MAb, 2G12,[4] which recognizes and requires an epitope comprising an Asn-linked oligomannose moiety.[13] Spurred by these findings, we conducted earlier two different NMR studies to determine whether discrete chemical shift perturbations, indicative of binding to a particular region on the protein, are observed for CVN in the presence of oligomannose or in the presence of recombinant SIV gp41. We found that under NMR conditions (~500 μM) CVN did not bind to $Man_5GlcNAc_2$ (Man_5) or $Man_7GlcNAc_2$ D1 (Man_7 D1), nor did it bind to the ectodomain of recombinant nonglycosylated SIV gp41[14] (Bewley, Caffrey, Clore, unpublished data), in agreement with findings by O'Keefe[10] and co-workers. However, in the presence of as little as 0.2 equiv of $Man_9GlcNAc_2$ (Man_9), CVN appeared to aggregate at NMR concentrations (Bewley, unpublished data). These observations, in combination with the dominance of N-linked glycosylation sites on gp120, suggested in particular a role for high mannose-type N-linked oligosaccharides in CVN−gp120 interactions.

Given the potential importance of CVN as a pharmacological agent for the prevention of transmission of HIV, we set out to design a series of experiments to determine the role of carbohydrates in the CVN−gp120 interaction as measured directly in a quantitative vaccinia virus-based HIV-1 envelope-mediated cell fusion assay and the structural requirements for carbohydrate recognition by CVN. To this end, we selected a comprehensive panel of oligosaccharides, the structures of which represent N-linked oligomannose-type and complex-type oligosaccharides present on gp120,[15] and tested their effect on the ability of CVN to block HIV-1 Env-mediated fusion. Our results demonstrate that CVN shows remarkable specificity and high affinity for particular biantennary and triantennary oligomannose structures emanating from the core Manβ1 unit (M3) and together with mapping of the carbohydrate binding sites on CVN provide the basis for a more detailed model of CVN−gp120 binding.

Results and Discussion

Carbohydrate Recognition by CVN As Determined in a Vaccinia Virus-Based Cell Fusion Reporter Gene Assay. To determine the nature of carbohydrate specificity of CVN, we used a quantitative vaccinia-virus based reporter gene assay[16] that directly measures the degree of HIV-1 envelope-mediated cell fusion between two cell populations, namely, effector cells that display HIV-1 envelope on their surface and target cells that have endogenous coreceptor CXCR4, via rates of β-galactosidase (β-gal) activity. Our rationale for using this approach was 2-fold: First, the propensity of CVN to aggregate at micromolar to millimolar concentrations in the presence of some oligomannose structures precluded detailed analysis of carbohydrate binding using traditional biophysical techniques in our earlier studies, and suggested that detailed binding studies be conducted at nanomolar concentrations. Second, because conflicting results have been reported in studies using different sources of gp120[4,5,9] (e.g., recombinant soluble gp120 vs fusion competent trimeric gp120 present on virus or cells, ref 17a, for example) we preferred to study the effects of carbohydrate binding to CVN in a biologically relevant system. The use of the cell fusion assay met both of these requirements as CVN inhibits HIV-1 envelope-mediated cell fusion at nanomolar concentrations and gp120 is present in a fusogenic state.

As previous studies have suggested a role for N-linked oligosaccharides in CVN−gp120 binding, we selected for screening a panel of 12 oligosaccharides (Figure 1b) that represent structurally the three classes of N-linked oligosaccharides present on gp120, namely, oligomannose-type ($Man_nGlcNAc_2$), asialo multiantennary complex-type (NA_n), and sialylated multiantennary-complex type (A_n) oligosaccharides. (We note that for simplicity we will refer to the various oligomannosyl-$GlcNAc_2$ structures simply as Man_n followed by isomer and branch designation if relevant.) As shown in Figure 2a, 100 nM CVN inhibits the relative rates of HIV-1 Env-mediated cell fusion by at least 90%, comparable to inhibition observed in other cell fusion studies.[5] In contrast, the oligosaccharides alone have no visible effect on fusion as relative rates are comparable to that of the positive control. In the right section of Figure 2a, results of fusion experiments using 100 nM CVN pretreated with a stoichiometric excess of oligosaccharide (in this case 200 nM) are shown. Neither the complex-type nor sialylated complex-type oligosaccharides effected the fusion-blocking activity of CVN, nor did Man_6, both isomers of Man_7, or the D1D2 isomer of Man_8. However, in the presence of either

(6) Bewley, C. A.; Gustafson, K. R.; Boyd, M. R.; Covell, D. G.; Bax, A.; Clore, G. M.; Gronenborn, A. M. *Nature Struct. Biol.* **1998**, *5*, 571−578.

(7) Yang, F.; Bewley, C. A.; Louis, J. M.; Gustafson, K. R.; Boyd, M. R.; Gronenborn, A. M.; Clore, G. M.; Wlodawer, A. *J. Mol. Biol.* **1999**, *288*, 403−412.

(8) Bewley, C. A.; Clore, G. M. *J. Am. Chem. Soc.* **2000**, *122*, 6069−6016.

(9) Mariner, J. M.; McMahon, J. B.; O'Keefe, B. R.; Nagashima, K.; and Boyd, M. R. *Biophy. Biochem. Res. Commun.* **1998**, *248*, 841−845.

(10) O'Keefe, B. R.; Shenoy, S. R.; Xie, D.; Zhang, W.; Muschik, J.; Currens, M. J.; Chaiken, I.; Boyd, M. R. *Mol. Pharmacol.* **2000**, *58*, 982−992.

(11) Mori, T.; Shoemaker, R. H.; Gulakowski, R. J.; Krepps, B. L.; McMahon, J. B.; Gustafson, K. R.; Pannell, L. K.; Boyd M. R. *Biochem. Biophys. Res. Commun.* **1997**, *238*, 218−222.

(12) Dedra, D.; Gu, R.; Tatner, L. *Virology* **1992**, *187*, 377−382. Douglas, N. W.; Munro, G. H.; Daniels, R. S. *J. Mol. Biol.* **1997**, *273*, 122−149.

(13) Trkola, A.; Purtscher, M.; Muster, T.; Ballaun, C.; Buchacher, A.; Sullivan, N.; Srinivasan, K.; Sodroski, J.; Moore, J. P.; Katinger, H. *J. Virol.* **1996**, *70*, 1100−1108.

(14) Caffrey, M.; Cai, M.; Kaufman, J.; Stahl, S. J.; Wingfield, P. T.; Covell, D. G.; Gronenborn, A. M.; Clore, G. M. *EMBO J.* **1998**, *17*, 4572−4584.

(15) Leonard, C. K.; Spellman, M. W.; Riddle, L.; Harris, R. J.; Thomas, J. N.; Gregory, T. J. *J. Biol. Chem.* **1990**, *265*, 10373−10382. Biller, M.; Bolmstedt, A.; Hemming, A.; Olofsson, S. *J. Virol. Methods* **1998**, *76*, 87−100.

(16) Salzwedel, K.; Smith, E.; Dey, B.; Berger, E. *J. Virol.* **2000**, *74*, 326−333. Nussbaum, O.; Broder, C. C.; Berger, E. *J. Virol.* **1994**, *68*, 5411−5422

(17) (a) Kwong, P. D.; Wyatt, R.; Sattentau, Q. J.; Sodroski, J.; Hendrickson, W. A. *J. Virol.* **2000**, *74*, 1961−1972. (b) Kwong, P. D.; Wyatt, R.; Robinson, J.; Sweet, R. W.; Sodroski, J.; Hendrickson, W. A. *Nature* **1998**, *393*, 648−659. (c) Wyatt, R.; Sodroski, J. *Science* **1998**, *280*, 1884−1888.

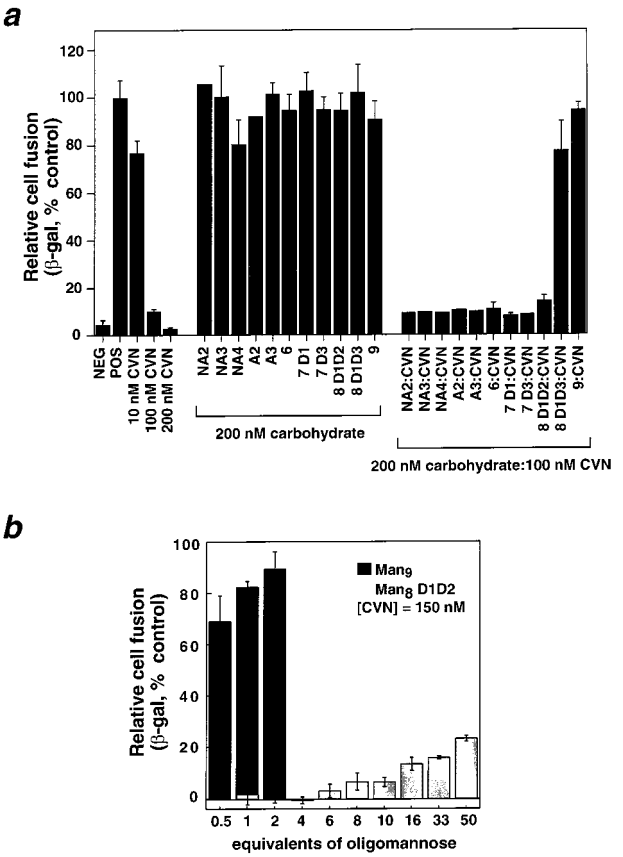

Figure 2. Effect of CVN and N-linked complex carbohydrates found on gp120 on HIV-1 Env-mediated cell fusion. (a) Controls and CVN inhibition are shown at left, the effect of carbohydrates alone at center, and effect of CVN when pretreated with the same panel of carbohydrates at right. Relative cell fusion was determined by measuring β-Gal activity where the positive control (absence of any inhibitors) was defined as 100%. The negative control (absence of CD4) is shown for comparison and was not subtracted from data shown. The mean observed values for positive and negative controls were $75 \pm 6 \times 10^{-3}$ OD/min and $1.3 \pm 0.04 \times 10^{-3}$ OD/min. All experiments were run at least in duplicate, and error bars indicate the standard deviation of the mean values for all experiments. Competition assays using CVN pretreated with oligomannoses were repeated at 5:1 stoichiometry yielding near identical results (data not shown). Labels 6, 7, 8, and 9 designate respective oligomannose-type oligosaccharides. (b) Titration of CVN with Man_8 D1D2. The first three corresponding points for treatment with Man_9 run in parallel are shown for comparison.

Man_8 D1D3 or Man_9 the fusion-blocking activity, and therefore gp120-binding, of CVN was nearly abolished. Thus Man_8 D1D3 or Man_9 can compete directly with gp120 for CVN binding.

The result that pretreatment of CVN with the D1D2 isomer of Man_8 failed to inhibit CVN−gp120 binding, while treatment with the structurally similar D1D3 isomer completely abrogated CVN−gp120 binding was quite surprising. To further test CVN binding to Man_8 D1D2, we treated CVN with increasing amounts of Man_8 D1D2 up to a 50-fold stoichiometric excess. As shown in Figure 2b, treatment of CVN with a 50-fold excess of Man_8 D1D2 restores fusion to the level of 25%, as compared to restoration of 80−90% upon pretreatment of CVN with only 1−2 equiv of Man_9. Thus, CVN specifically recognizes Man_8 D1D3 and Man_9 (see below for further discussion).

Binding of CVN to gp120, Man_8 D1D3, and Man_9. To investigate the binding affinity between CVN and gp120 expressed on effector cells, and between CVN and Man_8 D1D3 and Man_9, titration experiments were carried out with CVN alone and with 80 nM CVN pretreated with increasing amounts of oligosaccharide, and relative rates of fusion were measured. Assuming that measured β-Gal activity is directly proportional to the concentration of active gp120, experimental data for the titration of CVN to gp120, that is HIV-1 Env, were fit by nonlinear least squares optimization to the activity relationship given by eqs 1 and 2 for one-independent site and two-independent site models, respectively, where K_a is the equilibrium association constant.

$$\% \text{ fusion} = 100/(1 + K_a[\text{CVN}]) \quad (1)$$

$$\% \text{ fusion} = 100/(1 + 2K_a[\text{CVN}] + K_a^2[\text{CVN}]^2) \quad (2)$$

As shown in Figure 3a, the CVN titration data fit better to a two-independent site model comprising two molecules of CVN per molecule of gp120 than to a single site model which gives systematic errors in the fit. (The standard deviations of the best-fit curves for the 1-site and 2-site models were 3.8% and 2.4%, respectively.) The fit to the two-independent site model yields an equilibrium association constant K_a of 2.4 ($\pm$ 0.1) $\times$ 10^7 M^{-1} with an IC_{50} of 17 nM (given by $(\sqrt{2}-1)/K_a$). Figures 3b and 3c show relative rates of fusion as a function of the addition of increasing amounts of Man_8 D1D3 or Man_9, respectively, to 80 nM CVN. The oligomannose competition experiments were fit according to the models shown in Scheme 1 and simultaneously with the CVN−gp120 activity relationship presented in eq 2.[18] In the case of Man_8 D1D3, the best-fit curves indicate that CVN binds to Man_8 D1D3 with a 2:1 stoichiometry (that is two molecules of CVN bind to one molecule of oligosaccharide) and yields a K_a of 5.4 ($\pm$ 0.4) $\times$ 10^7 M^{-1}. (The standard deviations of the Man_8 D1D3 fits were 6.25% and 2.8% for one- and two-independent site models, respectively.) Data for titration of Man_9 to CVN is shown in Figure 3c where best fitting indicates a 3:1 stoichiometry for CVN to Man_9 (that is three molecules of CVN bind to one molecule of Man_9) and yields a K_a of 1.3 ($\pm$ 0.3) $\times$ 10^8. (The standard deviations of the Man_9 fits were 16%, 8.5%, and 4.8% for one-, two-, and three-independent site models, respectively.)

The stoichiometry of binding indicated by these fits is consistent with the respective biantennary and triantennary structures of Man_8 D1D3 and Man_9. Moreover, these results are gratifying since although cell fusion is essentially restored by pretreatment of CVN with stoichiometric amounts of either Man_8 D1D3 or Man_9, the data clearly show that fusion is restored more efficiently upon pretreatment with Man_9 than with Man_8 D1D3 (Figures 3b,c), indicating stronger avidity between CVN and Man_9. To view the differing stoichiometries of CVN binding to Man_8 or Man_9 more clearly, we have plotted the concentrations of bound CVN (obtained directly from the activities shown in Figures 3a−c as described in the figure legend) as a function of increasing oligomannose concentrations as shown in Figure 3d. This plot clearly shows a stoichiometry greater than 1 for CVN binding to either oligomannose and that more CVN is bound by equivalent concentrations of Man_9 than by Man_8 D1D3. For example, ~40 nM CVN is bound by 20 nM Man_8 D1D3, while ~60 nM CVN is bound by 20 nM Man_9.

Characterization of CVN−Oligomannose Binding at Micromolar Concentrations. In contrast to binding observed at nanomolar, i.e., biologically relevant, concentrations, the results of several experiments conducted using micromolar concentra-

(18) The factors of 2 and 3 in the 2-site and 3-site models originate from the number of discrete complexes that can be formed in each case. Thus, in the case of the 1:1 CVN:Man complex of the 2-site model (referred to as complex 1), CVN can be bound to either of 2 sites; for the 3-site model, CVN can be bound to any one of 3 sites in the 1:1 complex (complex 1), or to any of three combinations of 2 sites in the 2:1 complex (complex 2).

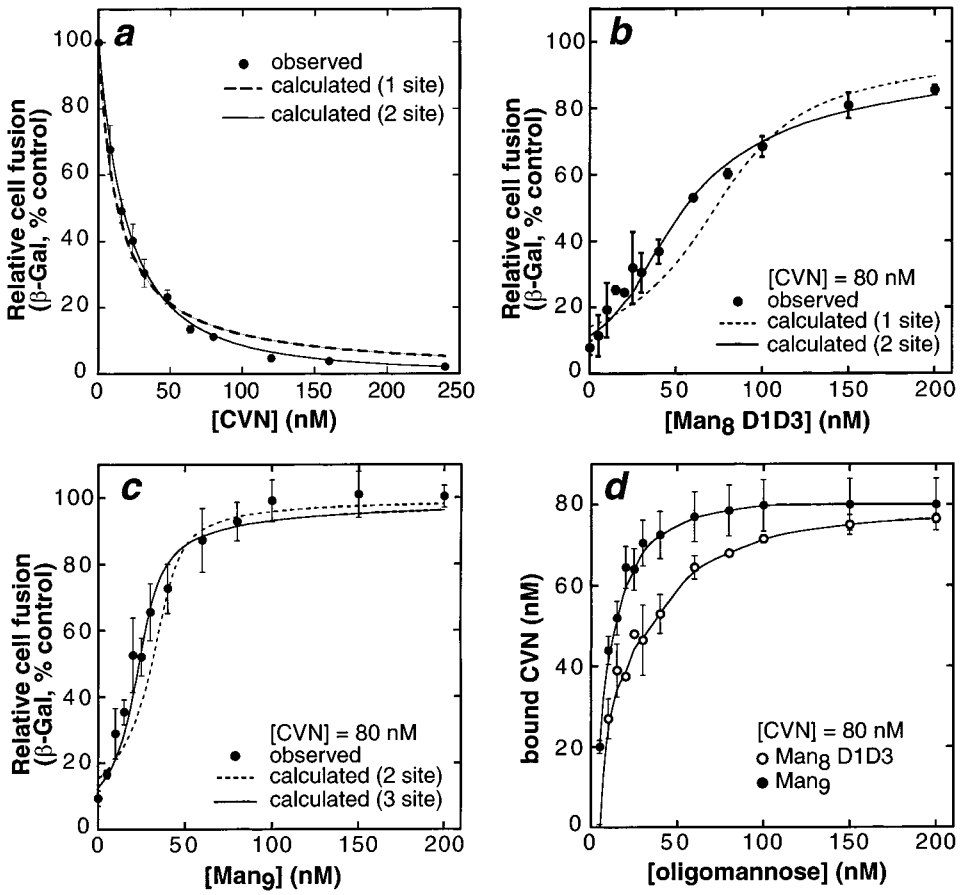

Figure 3. Binding studies of CVN to gp120, Man-8 D1D3 and Man-9 measured by effect on cell fusion. The effect on cell fusion of (a) increasing concentrations of CVN and CVN (80 nM) pretreated with increasing concentrations of (b) Man_8 D1D3 and (c) Man_9. (d) Plot of bound CVN versus oligomannose concentration deduced from the data in (a−c) in which % fusion is converted to concentration of unbound CVN and then to concentration of bound CVN from $[CVN_{bound}] = [CVN_{total}] - [CVN_{unbound}]$. In (a−c) the best fit curves obtained by nonlinear least squares optimization (described in the Experimental Section) to the experimental data (shown in solid circles) are shown as solid and dotted lines where the solid lines indicate the curves for the best-fitting model in each case as indicated in the plot. For CVN−gp120 and CVN−Man_8 D1D3, only the two-independent site model fits the data adequately with $K_a = 2.4 (\pm 0.1) \times 10^7\ M^{-1}$ and $5.4 (\pm 0.4) \times 10^7\ M^{-1}$, respectively, and for CVN−Man_9 the data fit best to a three-independent site model yielding $K_a = 1.3 (\pm 0.3) \times 10^8\ M^{-1}$. In (d) smooth curves are drawn to guide the eye.

tions of CVN and Man_8 D1D3 or Man_9 indicate that at these higher concentrations oligomerization occurs concomitant with complex formation. This behavior can be seen clearly in the native gels shown in Figures 4a and b. In the presence of 0.1−0.2 equiv of oligomannose, 2:1 CVN:oligomannose complexes are formed; however, upon further addition of oligomannose to CVN, oligomerization occurs. Similarly, NMR titration studies using a 150 μM sample of uniformly labeled ^{15}N-CVN showed that after the addition of 0.3−0.4 equiv of Man_8 D1D3, peaks were broadened to the extent that most were no longer visible, indicating formation of high molecular weight aggregates (see Supporting Information).

In a separate experiment to evaluate the binding of CVN to Man_9 at micromolar concentrations, isothermal titration calorimetry (ITC) measurements were performed wherein 3 μL aliquots of 800 μM Man_9 were added to 40 μM CVN until a molar ratio of 2 was reached (data provided in Supporting Information). A least squares best fit of the ITC data using a 1-site model yields an equilibrium association constant of $1.5 (\pm 0.9) \times 10^8\ M^{-1}$, an enthalpy of binding (ΔH) of −25.0 kcal M^{-1}, and, surprisingly, an apparent stoichiometry of approximately 1. The measured binding constant is in excellent agreement with that determined by nonlinear least squares fitting of the titration data obtained with the fusion assay and validates this approach to screening and quantifying protein−ligand binding. The finding that the ITC data yield a stoichiometry of 1 is revealing. To meet this requirement ($n = 1$), stoichiometric binding between CVN and Man_9 must be occurring under these conditions. Since we have already shown that at nanomolar concentrations CVN binds to Man_8 D1D3 and Man_9 with stoichiometries of 2 CVN:1 Man_8 and 3 CVN:1Man_9, respectively, the ITC results suggested that at micromolar concentrations or higher CVN binding to a divalent or trivalent ligand results in efficient cross-linking to yield a 1:1 complex. (If complexes comprising 2:1 or 3:1 CVN:oligomannose were formed as they are at nanomolar concentrations when CVN is present in excess of oligosaccharide, the results of best-fitting of the ITC data would be predicted to yield stoichiometries of 2 or 3, respectively. The data could not be fit using these stoichiometries.) Furthermore, the occurrence of cross-linking suggests that at least two carbohydrate binding sites must be present on CVN. The observed large negative enthalpy of binding suggests that CVN−carbohydrate binding is mediated predominantly by polar or electrostatic protein−ligand interactions as opposed to hydrophobic interactions, as would be expected given the polar nature of the ligand.

CVN Has Two Distinct Carbohydrate Binding Sites. In an effort to locate and characterize the carbohydrate binding sites on CVN, the following experiments were carried out. The finding that CVN specifically recognizes with nanomolar affinity Man_8 D1D3 and Man_9 suggested that a disaccharide comprising the Manα1 → 2Manα terminus or a trisaccharide comprising

Scheme 1[18]

1-site: CVN + Man $\underset{k_{-1}}{\overset{k_1}{\rightleftharpoons}}$ complex

2-site: CVN + Man $\underset{k_{-1}}{\overset{2k_1}{\rightleftharpoons}}$ complex1

CVN + complex1 $\underset{k_{-1}}{\overset{k_1}{\rightleftharpoons}}$ complex2

3-site: CVN + Man $\underset{k_{-1}}{\overset{3k_1}{\rightleftharpoons}}$ complex1

CVN + complex1 $\underset{k_{-1}}{\overset{3k_1}{\rightleftharpoons}}$ complex2

CVN + complex2 $\underset{k_{-1}}{\overset{k_1}{\rightleftharpoons}}$ complex3

$K_a = k_1/k_{-1}$

Man = oligomannose

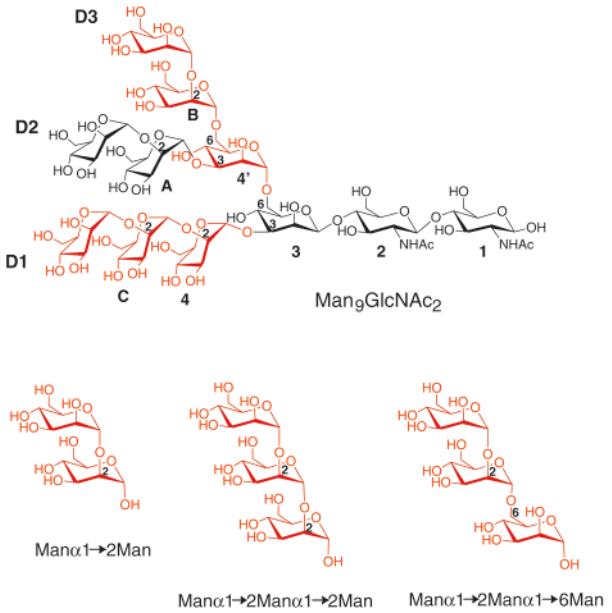

Figure 5. Chemical structures of oligosaccharides used in this study. Oligomannose structures are labeled by name and individual pyrannose rings and branches of Man_9 are labeled using standard nomenclature; the D1 and D3 arms of Man_9 and their corresponding di- and trisaccharides are colored red, and carbons are numbered to indicate the relevant 1 → 2 and 1 → 6 linkages.

all three mannose units of the D1 or D3 arms, namely, Manα1 → 2Manα1 → 2Manα or Manα1 → 2Manα1 → 6Manα, would present the requisite structures for high affinity binding to CVN (see Figure 5). Moreover, in terms of binding to CVN we surmised that these di- or trisaccharides would be monovalent ligands and should therefore preclude protein−oligosaccharide cross-linking and would thus be a good choice for probing the location of the putative dual carbohydrate binding sites on CVN by NMR. Due to the commercial availability of Manα1 → 2Man, this disaccharide was used in the NMR titration experiments. As shown in Figure 6a, a comparison of the $^1H-^{15}N$ correlation spectra at 500 MHz of free ^{15}N-CVN vs ^{15}N-CVN in the presence of 1 equiv of Manα1 → 2Man shows that addition of the disaccharide significantly perturbs a distinct set of chemical shifts comprising backbone amide protons for 18 residues. Moreover, two sets of peaks corresponding to free and bound CVN can be seen in the spectrum recorded in the presence of 0.5 equiv of Manα1 → 2Man, indicating that the complex is in slow exchange on the NMR time scale (spectrum provided in Supporting Information). As shown in Figure 6b, addition of a second equivalent of disaccharide causes a separate set of resonances to change, either slightly in chemical shift (in the case of G2, T7, C8, G96, and L98) or by line broadening due to intermediate chemical exchange on the NMR time scale (in the case of K3, F4, R24, T25, N26, I94, and D95). These results unambiguously demonstrate that CVN has two distinct carbohydrate binding sites. Moreover, for resonances residing in the first binding site, no further chemical shift changes are observed upon addition of greater than 1 equiv of disaccharide, indicating that the first site to be occupied binds to Manα1 → 2Man with significantly higher affinity than the second. We distinguish these sites by referring to them as the high affinity site and low affinity site, respectively. Upon addition of Manα1 → 2Man, the smallest chemical shift change ($\Delta\delta$) observed for resonances in the high affinity site is 4.9 Hz for Gln78 (NH) and the largest chemical shift change for resonances residing in the low affinity site is 36 Hz for Gly96(NH). Thus the lifetime of the CVN−Manα1 → 2Man complex bound through the high

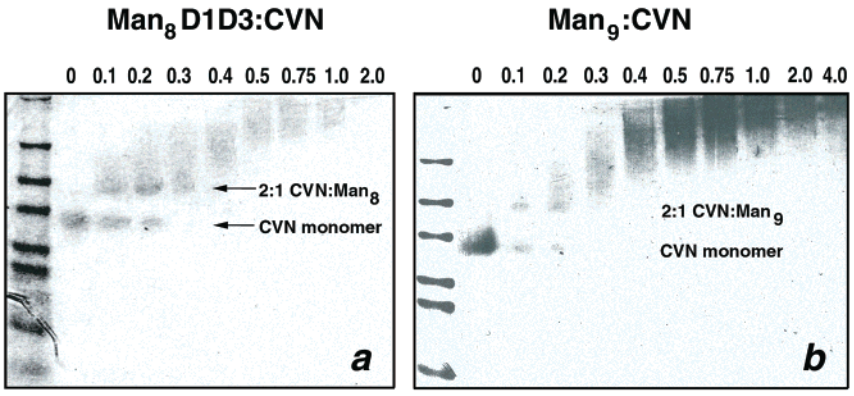

Figure 4. CVN−oligomannose binding at micromolar concentrations. Native gel electrophoresis showing formation of 2:1 and then higher order complexes of CVN and oligomannose upon titration with (a) Man_8 D1D3 and (b) Man_9; total equivalents of oligosaccharide are indicated above the gels.

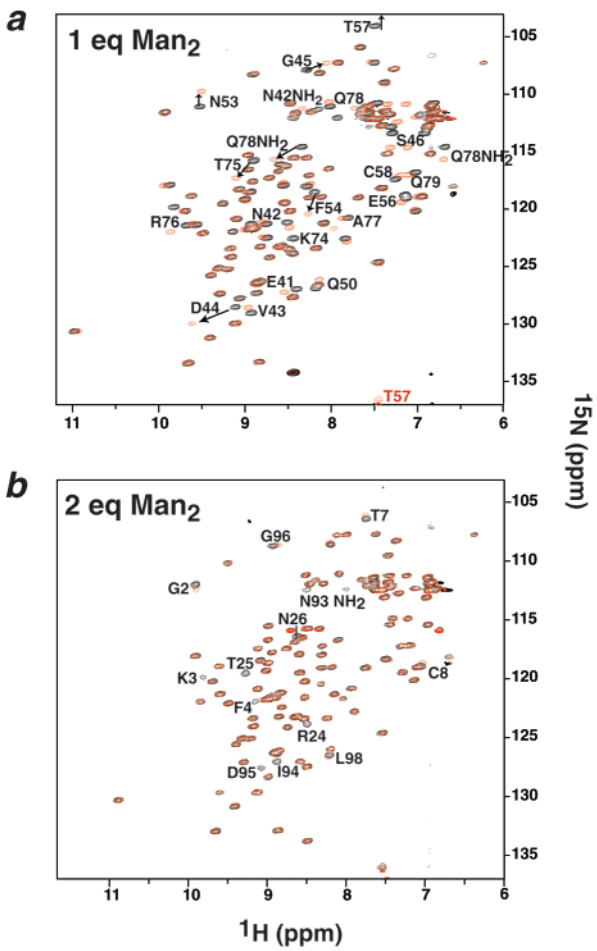

Figure 6. NMR titration of CVN with Man1 → 2Man. $^{1}H-^{15}N$ correlation spectra showing changes in chemical shifts of ^{15}N-CVN upon addition of (a) 1 equiv of Manα1 → 2Man, abbreviated in the figure as Man_2 and (b) 2 equiv of Manα1 → 2Man. In (a) spectra of CVN in the presence of zero and 1 equiv of Man_2 are shown in black and red, respectively, and in (b) CVN in the presence of 1 and 2 equiv of Man_2 are shown in black and red, respectively. Resonances that shift with addition of Man_2, or in the case of (b) those that broaden due to intermediate exchange on the NMR time scale, are labeled.

affinity site is ≫32.5 ms $[(2\pi\Delta\delta)^{-1}]$ while that for the complex bound through the low affinity site is ≤4.4 ms.

To determine the binding affinities of the individual sites, ITC experiments were conducted for CVN and Manα1 → 2Man disaccharide (Figure 7). The data were fit by least squares optimization to a two-independent site model, yielding K_a values of 7.2 (± 4) × 10^6 M^{-1} for the high affinity site and 6.8 (± 4) × 10^5 M^{-1} for the low affinity site, thus confirming the NMR results that demonstrated the presence of two binding sites with differing affinities. The data could not be fit adequately to a 1-site model.[19] (We note the binding affinities determined for this disaccharide may differ from those of the individual sites binding to a trisaccharide representative of the D1 or D3 arms of Man_8 D1D3 or Man_9.)

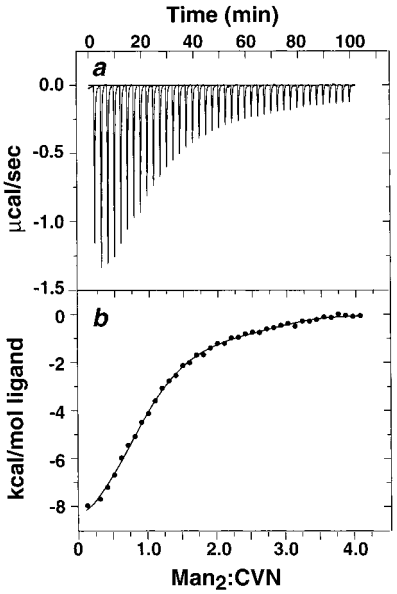

Figure 7. Isothermal titration calorimetry of CVN with Man1 → 2Man. (a) Raw data for 40 3 μL injections of Manα1 → 2Man to CVN as a function of time. (b) Plot of total heat released as a function of the molar ratio of Manα1 → 2Man to CVN and the best-fit curve generated from nonlinear least squares optimization. The data fit best to a two-independent site model which yields respective values for K_a and ΔH of 7.2 (±4) × 10^6 M^{-1} and −10.4 kcal M^{-1} for the high affinity site and 6.8 (±5) × 10^5 M^{-1} and −0.3 kcal M^{-1} for the low affinity site.

Discussion

In the studies described in this paper we have shown using a vaccinia virus-based fusion assay that CVN binds to fusogenic gp120, thereby inhibiting HIV-1 Env-mediated fusion with a K_a of 2.4 (± 0.1) × 10^7 M^{-1} and an apparent stoichiometry of 2 equiv of CVN to gp120.[20] NMR titration and ITC experiments using the disaccharide Manα1 → 2Man, which corresponds to the terminal pyranose rings of the D1 and D3 arms of the high affinity ligands Man_8 D1D3 and Man_9, revealed the presence of two carbohydrate binding sites with differing affinities (K_as of 7.2 (±4) × 10^6 M^{-1} and 6.8 (±4) × 10^5 M^{-1}) located on opposite end of the protein. Competition experiments using the fusion assay show that at nanomolar concentrations CVN binds to the divalent oligosaccharide Man_8 D1D3 and the trivalent oligosaccharide Man_9 through the high affinity site, with observed stoichiometries of 2 CVN:1 Man_8 D1D3 and 3 CVN:1 Man_9. It is only at micromolar to millimolar concentrations that CVN also binds oligomannose through the low affinity site, which accounts for the observed cross-linking at these higher concentrations. When these findings are considered together with the three-dimensional structures of CVN and Man_8 D1D3 or Man_9, and the locations of the carbohydrate binding sites, a more detailed structural model for CVN binding to gp120 emerges.

CVN is an 11 kDa monomeric protein that has a simple yet novel fold displaying C_2 pseudo-symmetry (Figure 1a).[6] The backside of the protein (as presented in Figures 1a and 8) comprises two adjacent triple-stranded antiparallel β sheets (β1−3 and β6−8), and the front of the protein comprises two opposing β-hairpins (β4, 5 and β9, 10). A single 3_{10}-helical turn connects each of these secondary structural elements. Due to the differing stoichiometries of CVN−oligosaccharide binding observed at nanomolar and micromolar concentrations, we

(19) We note that competition experiments employing Manα1 → 2Man were performed using the fusion assay, but the disaccharide was not able to compete with the several orders of magnitude greater affinity observed for the binding of CVN to gp120. Given the small size of CVN, and the lack of any additional polar binding sites sufficient to accommodate the extensive protein−carbohydrate interactions necessary for high affinity binding, we believe that oligomannose binds to CVN through the same binding sites as the disaccharide.

(20) We wish to make clear that this result does not eliminate the possibility of subsequent binding of additional CVN molecules to gp120 (O'Keefe et al. recently reported a stoichiometry of 5:1 for CVN binding to recombinant soluble glycosylated gp120[10]); instead it indicates that 2 equiv of CVN binding to gp120 is sufficient to inhibit fusion.

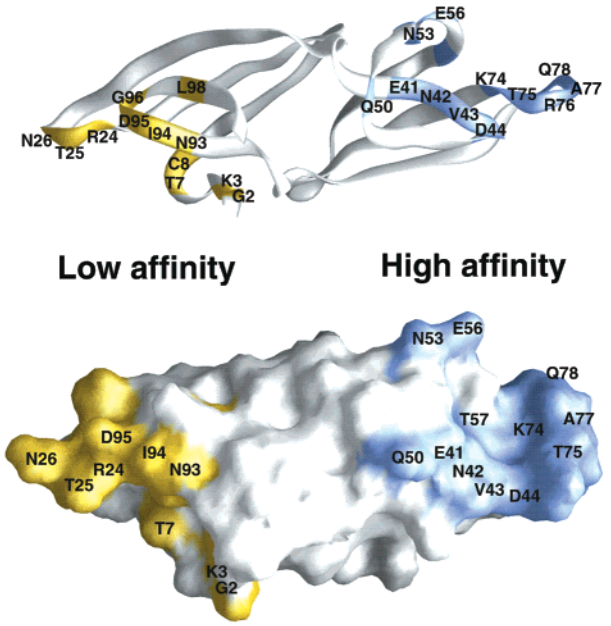

Figure 8. Map of the carbohydrate binding sites of CVN. (a) Backbone worm and (b) surface representations of CVN where residues comprising the high affinity and low affinity sites are colored light blue and yellow, respectively; residues that were perturbed in the NMR titration experiments and are visible in the views presented are labeled; figure was generated with the program GRASP.[36]

anticipated that CVN would possess two carbohydrate binding sites to accommodate cross-linking at micromolar concentrations or higher. In addition, the observed stoichiometries suggested that these sites would be separated by a distance greater than that separating the terminal pyranose rings of the D1 and D3 arms of Man_8 D1D3 and Man_9, that is >18 Å. Given the dimensions of CVN of ~25 Å across and 55 Å in length, this restraint further suggested that the binding sites would be located at opposing ends of the long axis of the protein. Indeed, if the latter were not the case, at nanomolar concentrations (that is concentrations less than or equal to the K_d for the binding of CVN to oligomannose) one would *not* expect formation of 2:1 or 3:1 CVN:oligomannose complexes as we observed in the fusion assay; instead, one would predict formation of 1:1 complexes wherein the two (or three) arms of one multivalent oligosaccharide molecule are bound to two (or more) separate sites of a single protein molecule. In addition to confirming the presence of two distinct carbohydrate binding sites, NMR titration studies using CVN and the disaccharide Manα1 → 2Man revealed the locations of the two binding sites which we have mapped onto the Cα worm and surface representations of CVN in Figure 8. Thus all of our expectations were met, and the distance separating the approximate centers of the two binding sites measures ~40 Å.

The presence of two carbohydrate binding sites on CVN separated by ~40 Å imposes certain structural restraints for CVN binding to gp120, a glycoprotein whose surface is largely covered by N-linked oligomannose structures,[17] and thereby presents a possible mechanism accounting for its ability to block Env-mediated fusion. First, given the presence of two carbohydrate binding sites with differing affinities, it is likely that CVN binds to oligomannose present on gp120 via the high affinity site. Once bound, CVN could further interact with proximal oligomannose units via the lower affinity site (due to the high apparent concentration of oligomannose once CVN is bound to gp120). If CVN binding to gp120 involves *both* carbohydrate binding sites, it follows that CVN will be bound to two separate oligomannose units on gp120 which would result in cross-linking of the envelope protein. In either case, CVN bound to gp120 may block chemokine receptor binding sites on gp120,[4,5] prevent subsequent conformational changes in the envelope protein that are required for viral fusion, or both. Second, we have shown that CVN binds to fusogenic gp120, Man_8 D1D3, and Man_9 with comparable low nanomolar affinities and pretreatment of CVN with these oligosaccharides abrogates the fusion-blocking activity of CVN. These results alone suggest that CVN binding to gp120 probably occurs solely through carbohydrate-mediated interactions. However, added steric considerations make this argument even more compelling. As shown in Figure 8, the two oligomannose binding sites on CVN are located on the same face of opposite ends of the protein. Binding to oligomannose units present on gp120 through both carboydrate binding sites will essentially fix the position of CVN parallel to the virus with the carbohydrate binding face directed toward gp120, leaving only the back face of CVN available for any other appreciable carbohydrate-independent interactions with gp120. Since the distance between the reducing end and the mannopyranose termini of Man_9 is approximately 25 Å (Figure 9), as is the distance across CVN, it is unlikely that after oligosaccharide binding CVN is able to approach the peptidic portion of gp120 for additional specific interactions. In light of these restraints, we propose that CVN binds to gp120 exclusively through oligomannose-mediated interactions.

We have shown that CVN specifically recognizes Man_8 D1D3 and Man_9 with nanomolar affinity but does not bind to any measurable degree Man_6, isomers of Man_7, or Man_8 D1D2. These results would appear to suggest that the optimal moeity for CVN recognition includes a terminal trisaccharide comprising Manα1 → 2Manα1 → 2/6Man (see Figure 5). However, our NMR titration experiments and ITC data using the terminal disaccharide unit Manα1 → 2Man demonstrate that CVN also binds to this disaccharide with low micromolar affinity. (The K_a of CVN binding to a relevant trimannosyl trisaccharide is unknown at this time.) Despite the presence of a terminal Manα1 → 2Man disaccharide in all oligomannose structures bearing the core Man_6 unit (Figures 1b and 5), CVN recognized only Man_8 D1D3 and Man_9 with high affinity. This observed specificity might suggest that high affinity binding requires more stringent structural features of the oligomannose than one would initially predict. For example, CVN−oligomannose binding might require the terminal disaccharide Manα1 → 2Man to be sterically unhindered, a structural requirement that is best met by Man_8 D1D3 and Man_9, or that the 1 → 2 or 1 → 6 linkages connecting the D1 and D3 arms to the oligomanose core adopt a specific conformation. In regard to steric considerations, the relative positions of the three arms of oligomannose can be better appreciated by considering the three-dimensional structures of Man_8 or Man_9. Stereoviews and surface representations of a representative low energy structure of Man_9 determined by molecular dynamics[21] (and in agreement with experimentally determined distance and dihedral angle restraints[21,22]) are presented in Figure 9 and show that while the D1 and D3 arms form a continuous and accessible surface, the 1 → 3 linkage of the D2 arm orients the disaccharide almost orthogonal to the long axis of the molecule and proximal to the core,[23] rendering it less accessible for binding. As for the notion that CVN binding

(21) Woods, R. J.; Pathiaseril, A.; Wormald, M. R.; Edge, C. J.; Dwek, R. A. *Eur. J. Biochem.* **1998**, *258*, 372−386

(22) Wooten, E. W.; Bazzo, R.; Edge, C. J.; Zamze, S.; Dwek, R. A.; Rademacher, T. W. *Eur. Biophys. J.* **1990**, *18*, 139−148.

(23) In fact Wooten et al.[22] observed NOEs between mannopyranose units of the D2 arm and the $GlcNAc_2$ core of Man_9.

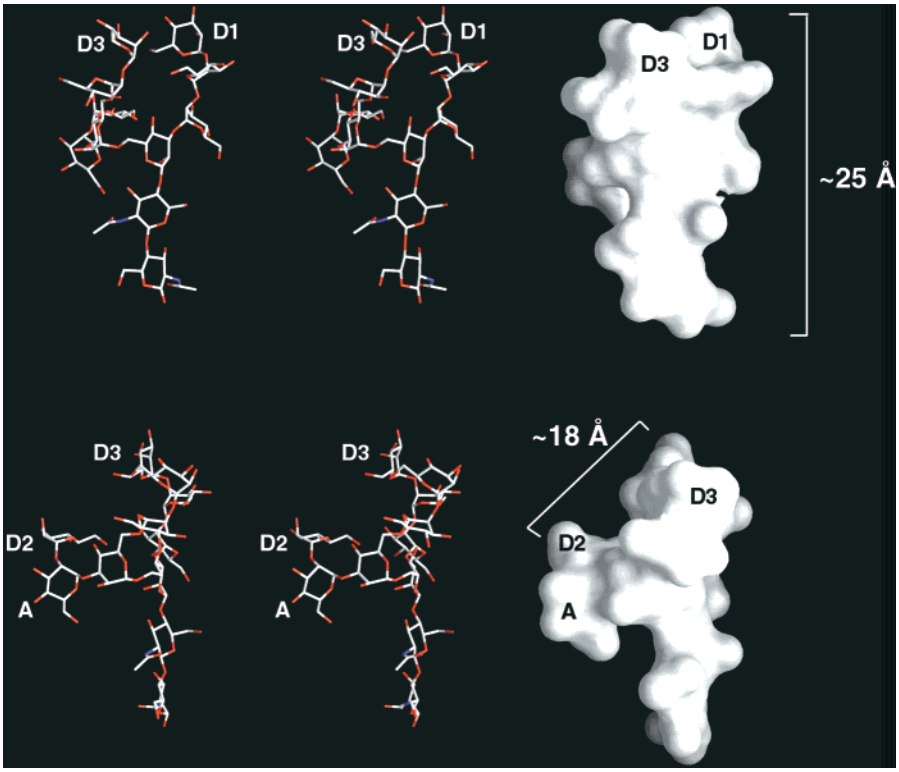

Figure 9. Structures of Man9GlcNAc2. Stereoview and surface representations of a low energy conformation of $Man_9GlcNAc_2$[21] showing a continuous and accessible surface presented by the D1 and D3 arms of Man_9; the bottom panel shows $Man_9GlcNAc_2$ after a 90° counterclockwise rotation about the *y*-axis from the orientation seen in the top panel; red and white bonds denote oxygen and carbon atoms, respectively. Figure was generated with the program GRASP.[36]

to oligomannose might require the dimannosyl or trimannosyl termini to adopt a specific conformation, it is interesting to note that the dihedral angles of the linkages connecting the D1, D2, and D3 arms of oligomannose to the core have been shown to vary depending on the substituents of the various arms.[22,24] (Such specificity must also occur with glycoprotein biosynthesis and oligosaccharide trimming.)

The phenomenon of lectin−oligosaccharide cross-linking has been studied extensively.[25] Most plant lectins exist as homodimers or tetramers and have a single carbohydrate binding region per monomer with binding affinities in the micromolar to millimolar range for monosaccharides and disaccharides. For these proteins, cross-linking occurs with a stoichiometry of 1:2 for divalent ligand:lectin monomer (or 1:1 for divalent ligand to lectin dimer). In the case of CVN, Nature has dispensed with the need for dimer or tetramer formation by artfully including internal 2-fold pseudo-symmetry and two homologous carbohydrate binding sites within a single protein molecule.[26] While synthetic multivalent ligands bearing mannopyranose termini and exhibiting nanomolar affinities toward mannose binding proteins such as MBP-A and concanavilin A have been constructed,[27] to the best of our knowledge this is the first detailed characterization of low nanomolar binding affinity between a mannose-specific protein and a naturally occurring oligosaccharide. We have surveyed the carbohydrate binding sites of crystal structures of mannose binding proteins for comparison to the mannose binding sites mapped on CVN. While we were able to identify a tetrad of opposing pairs of asparagine and glutamate residues (namely, Asn42, Asn53, Glu41, and Glu56) poised in a nearly identical arrangement to that seen in the carbohydrate binding pocket of mannose binding protein A,[28] an animal lectin that in contrast to CVN requires Ca^{2+} for activity,[29] no other previously reported mannose binding motifs are present. Thus CVN binds to mannopyranose moieties using a novel and extensive (in the case of the high affinity site at least 18 residues are involved) carbohydrate binding interface, the details of which will be revealed with a high resolution structure of a CVN−oligomannose complex.

In closing, given that CVN certainly exerts its strong antiviral activity through high affinity interactions with oligomannose residues present on surface envelope glycoproteins, it is interesting to note that CVN does not inhibit all enveloped viruses thus far tested.[3,5] In addition to its promise as a topical antiviral agent for the prevention of sexual transmission of HIV, several other uses for CVN come to mind: CVN may prove to be a powerful research tool to aid investigators studying the structure and conformational changes of enveloped virus coat proteins and

(24) Petrescu, A. J.; Butters, T. D.; Reinkensmeier, G.; Petrescu, S.; Platt, F. M.; Dwek, R. A.; Wormald, M. R. *EMBO J.* **1997**, *16*, 4302−4310.

(25) (a) Mandal, D. K.; Brewer, C. F. *Biochemistry* **1992**, *31*, 12602−12609. (b) Brewer, C. F. *Chemtracts Biochem. Mol. Biol.* **1996**, *6*, 165−179. (c) Bourne, Y.; Bolgiano, B.; Liao, D.; Strecker, G.; Cantau, P.; Herzberg, O.; Feizi, T.; Cambillau, C. *Nat. Struct. Biol.* **1994**, *1*, 863−869.

(26) Note that the cross-linking observed for CVN-oligomannose does not discount the possibility that carbohydrate-*independent* dimerization or oligomerization of CVN occurs concomitant with carbohydrate-mediated cross-linking, but we have never observed the formation of homodimers nor oligomers of free CVN during extensive NMR and biophysical studies. The observation that CVN can partially unfold in the presence of organic solvents to form a domain-swapped dimer[7,8] is unrelated to the 2:1 or 3:1 monomeric CVN:oligomannose complexes observed here.

(27) (a) Dimick, S. M.; Powell, S. C.; McMahon, S. A.; Moothoo, D. N.; Naismith, J. H.; Toone, E. J. *J. Am. Chem. Soc.* **1999**, *121*, 10286−10296. (b) Page, D.; Zanini, D.; Roy, R. *Bioorg. Med. Chem.* **1996**, *4*, 1949−1961. (c) Quesenberry, M. R.; Lee, R. T.; Lee, Y. C. *Biochemistry* **1997**, *36*, 2724−2732. General reviews by the following. (d) Mammern, M.; Choi, S.; Whitesides, G. M. *Angew. Chem., Int. Ed.* **1998**, *37*, 2754−2794. (e) Kiessling, L. L.; Pohl, N. L. *Chem. Biol.* **1996**, *3*, 71−77.

(28) Weis, W. I.; Drickamer, K.; Hendrickson, W. A. *Nature* **1992**, *360*, 127−134.

(29) Drickamer, K. *Cur. Opin. Struct. Biol.* **1999**, *9*, 585−590.

may find great utility as a reagent for specifically selecting and purifying Man_8 D1D3- and Man_9-containing molecules. Finally, a high resolution structure of the novel, high affinity oligomannose binding site in complex with mannopyranose may serve as a template for future design of high affinity mannose binding proteins and artificial receptors.

Experimental Section

Cells. Human HeLa cells (American Type Culture Collection) grown in Dulbecco-modified Eagle medium supplemented with 10% fetal bovine serum (DMEM 10%), 2 mM L-glutamine, and gentamycin at 50 μg/mL (all from Gibco BRL, Bethesda, MD) were used for all assays.

Reagents. Recombinant vaccinia viruses used in this study include vCB41,[30a] vP11T7gene1,[30b] and vCB21R-LacZ, which encode HIV-1 LAV Env (T-cell line tropic), bacteriophage T7 RNA polymerase driven by a vaccinia virus promoter, and the *Escherichia coli lacZ* gene under control of the T7 promoter, respectively. Two-domain soluble CD4 (1−183) was a gift from E. Berger (NIAID, NIH) and donated by S. Johnson (Pharmacia Upjohn, Kalamazoo, MI). Recombinant CVN was expressed either as previously described,[6] or using a synthetic gene encoding amino acids gly-(1−101) of CVN inserted into pET-11 (Novagen) with expression in Origami cells (Stratagene) to promote disulfide formation, followed by purification using reversed-phase HPLC (C18, YMC) and gel-filtration (Superdex 75, Amersham Pharmacia) to ensure separation of monomeric and domain-swapped dimeric[7] CVN, which are present at a ratio of ~90:10. Oligosaccharides used in this study were purchased from Glycotech, Inc. (Rockville, MD), Glyko, Inc. (Novato, CA), or Sigma-Aldrich (St. Louis, MO) and were >95% pure as judged by mass spectrometry and ^{1}H NMR of each product. Stock solutions of protein and oligosaccharides were prepared in phosphate buffered saline, pH 7.4 (PBS). Chlorophenol-red-β-D-galactopyranoside (CPRG) was purchased from Roche.

Cell Fusion Assays. A modification of the vaccinia virus-based reporter gene assay employing soluble CD4 (200 nM final concentration) was used to determine the effect on HIV Env-mediated cell fusion of CVN and/or oligosaccharides, and assays were conducted as described by Salzwedel et al.[16] Briefly, HeLa cells (which have endogenous CXCR4) were used for both target cell and effector cell populations, where target cells were infected with vCB21R-LacZ, and effector cells coinfected with vCB41 and vP11T7gene1, at an MOI of 10. For inhibition studies and controls, CVN or oligosaccharides were added to an appropriate volume of DMEM 2.5% and PBS to yield identical buffer compositions (100 μL), followed by addition of 1×10^5 effector cells (in 50 μL media) per well. After a 15 min incubation, 1×10^5 target cells (in 50 μL) and soluble CD4 were added to each well. Following a 2.5 h incubation, β-galactosidase activity of cell lysates was measured (A570, Molecular Devices 96-well spectrophotometer) upon addition of CPRG. Competition experiments were performed with the modification that CVN and oligosaccharide were combined prior to addition of effector cells. All experiments were run in duplicate on at least three separate occasions. CVN titrations were carried out in parallel with all competition experiments, and data always fit the two-independent site model described in the text. Competition experiments were carried out using both a 2-fold (Figure 2a) and 5-fold (data not shown) stoichiometric excess of each of the carbohydrates.

Nonlinear Least Squares Optimization of Titration Data. Since the concentrations of CVN and oligomannose are comparable in the competition experiments, the concentration of the various species in Scheme 1 were determined numerically by integration to a time point (1000 s) at which full equilibrium had been reached. Computations were carried out using the program FACSIMILE[31] that makes use of Powell's method of nonlinear optimization and a modified Gear method for numerical integration.

Gel Electrophoresis. CVN−oligosaccharide complexes were formed by adding appropriate quantities of Man_8 D1D3 or Man_9 to solutions containing 2.5 μM (~550 ng/20 μL final volume) monomeric CVN (confirmed by a ^{1}H−^{15}N heteronuclear correlation spectrum[8] and gel filtration[7]) in PBS, pH 7.4. Complexes were loaded onto 10−20% Tris-Glycine gels (Novex, Invitrogen) and run under native conditions (no sodium dodecyl sulfate, 120 V) for ~2 h. It should be noted that CVN is a highly elongated protein measuring ~55 Å in length with a maximum width of ~25 Å and therefore runs with an apparent molecular weight of ~45 kDa under native conditions. Furthermore, although a 2:1 CVN:oligosaccharide complex will be less elongated relative to its total mass than free CVN, such a complex is still far from globular. Thus slower migration, or higher apparent molecular weight, in the native gel would also be expected for the 2:1 complex and is observed as it runs with an apparent molecular weight of ~60 kDa.

Isothermal Titration Calorimetry Measurements of Oligomannose−CVN Binding. ITC measurements and analysis were performed with a Microcal Omega titration calorimeter and Origin software as described previously.[32] In each experiment, 1.35 mL of 30−40 μM CVN was present in the solution cell and 20−40 3−5 μL aliquots of ligand were added via a 250 μL rotating stirrer-syringe every 150 s. The ligands included solutions of 700 μM Man_9, 1.3 mM Manα1 → 2Man, 700 μM α-D-mannose, and 20 mM α-D-mannose (to ensure saturation should the monosaccharide be able to bind nonspecifically if present in great excess). All solutions were made with 10 mM Tris buffer, pH 6.5, and measured at 25 °C. Controls were performed for each experiment wherein the appropriate ligand solution was added to buffer in the absence of CVN. In the case of α-D-mannose and CVN, the binding isotherms were indistinguishable from those of the controls, indicating that no binding occurs with the monosaccharide. Similar experiments were not conducted with Man_8 due to lack of material.

NMR Spectroscopy. NMR experiments were performed on Bruker DMX500 and DMX600 spectrometers equipped with *x,y,z*-shielded gradient triple resonance probes. Uniformly labeled ^{15}N-CVN used in NMR experiments was expressed as described in Reagents section above, with the exception that *E. coli* were grown in minimal media with $^{15}NH_4Cl$ as the sole nitrogen source. Titration experiments were performed as follows: ^{1}H−^{15}N correlation spectra were recorded on (a) a 250 μL sample of 0.15 mM ^{15}N-CVN in the presence of 0, 0.1, 0.2, 0.3, and 0.4 equiv of Man_8 D1D3 where ligand was added in 10 μL aliquots or (b) a 0.5 mM ^{15}N-CVN sample in the presence of 0, 0.5, 1.0, 1.5, 2.0, 2.5, 3.0, 3.5, and 4.0 equiv of Manα1 → 2Man where ligand was added in 5 μL aliquots. All solutions were prepared in 10 mM $NaPO_4$ and the pH was adjusted to 6.2. For the oligomannose titrations, Man_8 D1D3 was chosen because oligomerization occurs to a lesser extent with Man_8 D1D3 than with Man_9 (at mM concentrations, gelatinous aggregates of CVN−Man_9 can form, unpublished data; spectra are provided in Supporting Information). Spectra were processed and peak volumes and heights measured using the software packages NMRPipe[33] and PIPP,[34] respectively.

Acknowledgment. We thank Edward Berger and Paul Kennedy for the generous gifts of recombinant vaccinia viruses and soluble CD4; Karl Salzwedel, Paul Kennedy, Barna Dey, and Edward Berger for numerous stimulating discussions regarding cell fusion; Michael Boyd and Toshi Mori for CVN-expressing plasmid used in earlier unpublished NMR studies; Marius Clore and Attila Szabo for helpful suggestions regarding

(30) (a) Broder, C. C.; Berger, E. *Proc. Natl. Acad. Sci. U.S.A.* **1995**, *92*, 9004−9008. (b) Alexander, W. A.; Moss, B.; Fuerst, T. T. *J. Virol.* **1992**, *66*, 2934−2942.

(31) References for the program FACSIMILE and its use include the following. (a) Curtis, A. R. U.K. Atomic Energy Research Establishment, 1980, Report No. R9352, Harwell. (b) Chance, E. M.; Curtis, A. R.; Jones, I. P.; Kirby, C. R. U.K. Atomic Energy Research Establishment, 1978, Report No. R8775, Harwell. (c) Clore, G. M. *Computing in Biological Science*; Geisow and Barrett: Amsterdam, 1983; pp 313−34.

(32) Schwartz, F. P.; Puri, K.; Bhat, R. G.; Surolia, A. *J. Am. Chem. Soc.* **1993**, *266*, 24344−24350, and references therein.

(33) Delaglio, F.; Grzesiek, S.; Vuister, G. W.; Zhu, G.; Pfeifer, J.; Bax, A. *J. Biomol. NMR* **1995** *6*, 277−293.

(34) Garrett, D. S.; Powers, R.; Gronenborn, A. M.; Clore, G. M. *J. Magn. Reson.* **1991**, *95*, 214−220.

(35) Koradi, R.; Billeter, M.; Wuthrich, K. *J. Mol. Graph.* **1996**, *14*, 29−32.

(36) Nichols, A.; Sharp, K. A.; Honig, B. *Proteins Struct. Funct. Genet.* **1991**, *11*, 281−296.

fitting of titration data; Kirk Gustafson and Barry O'Keefe for many interesting discussions regarding CVN activity; Mark Wormald and Raymond Dwek for $Man_9GlcNAc_2$ coordinates; and Marius Clore for many fruitful discussions and along with anonymous reviewers a critical reading of the manuscript. This work was supported in part by the Intramural AIDS Targeted Antiviral Program of the Office of the Director, National Institutes of Health.

Supporting Information Available: Isothermal titration calorimetry data for CVN−Man_9 titration; overlay of the $^1H-^{15}N$ correlation spectra of CVN recorded in the presence of 0 and 0.3 equiv of $Man_8GlcNAc_2$ D1D3, and $^1H-^{15}N$ correlation spectrum of CVN in the presence of 0.5 equiv of Manα1 → 2Man. This material is available free of charge via the Internet at http://pubs.acs.org.

JA004040E